

# Extension of tunable far-infrared spectroscopy to 7.9 THz

Hitoshi Odashima

Department of Physics, Toyama University, Gofuku 3190, Toyama 930, Japan

Maki Tachikawa, Lyndon R. Zink, and Kenneth M. Evenson

Time and Frequency Division, National Institute of Standards and Technology, 325 Broadway, Boulder, Colorado 80303

Received February 18, 1997

We generated tunable far-infrared radiation by mixing CO<sub>2</sub>-laser, <sup>15</sup>NH<sub>3</sub>-laser, and microwave radiations in a W-Co metal-insulator-metal diode. We used this far-infrared radiation to measure accurately the torsion-rotation transitions of CH<sub>3</sub>OH in the 6–8-THz region.

In the 5–10-THz region of the far infrared (FIR), high-resolution spectroscopy is difficult because tunable, coherent radiation is difficult to produce.<sup>1</sup> Although Fourier-transform spectroscopy covers this region, its typical resolution is ~50 MHz, and its accuracy is limited to ~3 MHz.<sup>2</sup> The powerful Schottky-diode “FIR laser plus microwave sideband” mixing technology<sup>3</sup> recently exploited for studies of weakly bound clusters,<sup>4</sup> molecular ions,<sup>5</sup> and carbon clusters<sup>6</sup> has not been extended beyond 4.5 THz and may be limited by the intrinsic capacitance of these mixers. In 1984 Evenson and co-workers invented a tunable far-infrared (TuFIR) spectrometer based on the difference frequency of two CO<sub>2</sub> lasers in a metal-insulator-metal (MIM) diode.<sup>7–9</sup> This method provides tunable, coherent FIR radiation with a frequency uncertainty of 14 kHz,<sup>10</sup> permitting measurement of FIR transition frequencies of atoms and molecules with an accuracy that depends generally on finding the center of the absorption line (for CH<sub>3</sub>OH, less than 100 kHz).<sup>11,12</sup> FIR transitions up to 6.5 THz were observed when an isotopic <sup>13</sup>CO<sub>2</sub> laser was used as one of the two CO<sub>2</sub> lasers and a regular <sup>12</sup>CO<sub>2</sub> laser was used as the other.<sup>11</sup> The maximum FIR frequency is limited by the maximum frequency difference between two CO<sub>2</sub> lasers.

To generate tunable, coherent radiation above 6 THz, we replaced one of the two CO<sub>2</sub> lasers in a traditional TuFIR spectrometer with an optically pumped, mid-infrared <sup>15</sup>NH<sub>3</sub> laser. Because the <sup>15</sup>NH<sub>3</sub> laser has several lines at lower frequencies (23–27 THz) (Ref. 13) than a <sup>13</sup>CO<sub>2</sub> laser has (26–31 THz),<sup>14</sup> difference frequencies up to 10 THz are possible.

A block diagram of the spectrometer is shown in Fig. 1. The ammonia laser is optically pumped by the *R*(42)<sub>I</sub> line of a CO<sub>2</sub> laser, which is coincident with the *aR*(2, 0) transition of <sup>15</sup>NH<sub>3</sub>. The pump laser power is ~18 W. A grating selects one of five <sup>15</sup>NH<sub>3</sub> laser lines, *aP*(4, 0), *aP*(4, 3), *aP*(5, 3), *aP*(6, 0), or *aP*(6, 3), with a typical power of 300–600 mW. More details of this laser are described elsewhere.<sup>15</sup> After passing through a 17-cm-long CH<sub>3</sub>OH absorption cell, which blocks any residual CO<sub>2</sub> laser radiation superposed upon the ammonia laser beam, the ammonia-laser output is split in half. The first half is used to stabilize the ammonia-laser frequency; the second half is used to generate FIR radiation.

The first half is double passed through a 17-cm-long absorption cell of <sup>15</sup>NH<sub>3</sub> at ~1.3 Pa (10 mTorr), and a saturation-dip signal is observed with a HgCdTe detector. A typical depth of the dip is ~15% of the absorption, and a typical width is a few megahertz. The ammonia laser is stabilized to the center of this dip, with its third-derivative signal used as an error signal.<sup>16,17</sup> This 3f servo technique gives the <sup>15</sup>NH<sub>3</sub> laser a frequency stability of 100–150 kHz, reducing a systematic frequency shift that is due to an asymmetric gain profile caused by cavity misalignment, off-resonance pumping, and other effects. The 3f-stabilized <sup>15</sup>NH<sub>3</sub> laser frequencies will be reported in Ref. 18.

The other half of the ammonia-laser radiation (frequency  $\nu_1$ ) is mixed with CO<sub>2</sub>-laser radiation ( $\nu_2$ ) in a W-Co MIM diode. This CO<sub>2</sub> laser is stabilized to the saturation dip in a 4.3-μm fluorescence signal of CO<sub>2</sub> with the traditional 1f servo technique.<sup>19</sup> The CO<sub>2</sub> reference frequencies are reported in Ref. 14. Typical incident powers are 150 mW for the CO<sub>2</sub> laser and 100–150 mW for the <sup>15</sup>NH<sub>3</sub> laser. Several milliwatts of microwave radiation from the synthesized sweeper ( $1 \leq \nu_{MW} \leq 20$  GHz) is also coupled onto the diode. The W-Co MIM diode generates two tunable

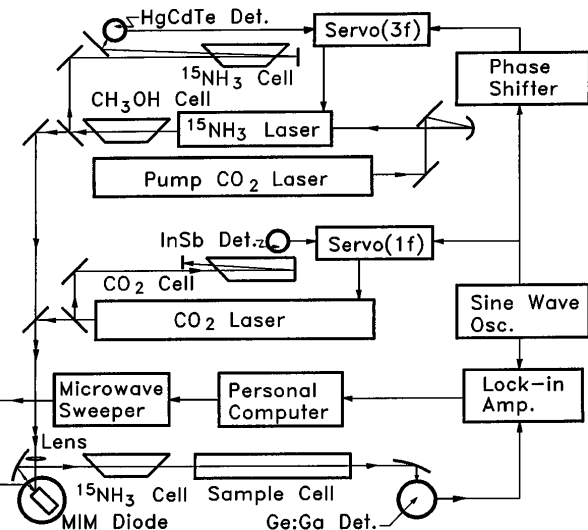


Fig. 1. Block diagram of the TuFIR spectrometer based on the difference frequency of CO<sub>2</sub> and <sup>15</sup>NH<sub>3</sub> lasers. Det's, detectors; Amp., amplifier; Osc., oscillator.

FIR frequencies equal to  $\nu_{\text{FIR}} = |\nu_1 - \nu_2| \pm \nu_{\text{MW}}$ . One changes the synthesized FIR frequency by tuning the microwave source. The generated FIR radiation is collimated with an off-axis parabola and sent through a 1.1-m-long sample cell with 80- $\mu\text{m}$ -thick polypropylene windows at both ends. It is then detected by a gallium-doped germanium (Ge:Ga) photoconductive detector with an 8–16- $\mu\text{m}$  diamond scatter filter used to reduce the IR radiation for  $\lambda < 14 \mu\text{m}$ . A 20-cm-long cell of  $^{15}\text{NH}_3$  at 133 Pa (1 Torr) is placed in front of the sample cell to eliminate any residual  $^{15}\text{NH}_3$  laser radiation. The frequencies of both lasers are modulated at 450 Hz with opposite phases for frequency stabilization; hence the generated FIR frequency is also modulated with an amplitude of a few megahertz. The detected signal is demodulated by a lock-in amplifier operated in the  $1/f$  mode. Both the microwave sweeper and the lock-in amplifier are computer controlled, and the first-derivative curve of the absorption is recorded on a computer.

$\text{CH}_3\text{OH}$  was chosen as a sample gas because of its rich torsion-rotation spectrum over 6 THz.  $\text{CH}_3\text{OH}$  pressure was  $\sim 1.3 \text{ Pa}$  (10 mTorr), and five transitions

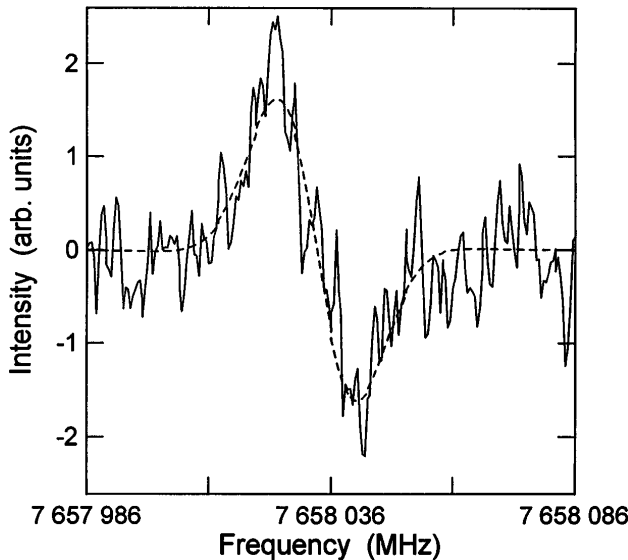


Fig. 2. Observed spectral line of the  $A (n, k, J) = (1, 5, 12) \leftarrow (0, 4, 11)$  transition of  $\text{CH}_3\text{OH}$  at 7.6 THz. The time constant of the lock-in amplifier is 300 ms. The measured spectrum is the solid curve, and the fitted spectrum is the dashed curve.

from 6 to 8 THz were measured. A plot of the observed absorption from the  $A (n, K, J) = (1, 5, 12) \leftarrow (0, 4, 11)$  transition at 7.6 THz is shown in Fig. 2, where  $n$  is the torsional quantum number. The observed transitions were assigned by reference to Fourier-transform spectrometer data.<sup>20</sup> The measured transition frequencies are listed in Table 1. They are the average of several measurements, and their  $1\sigma$  uncertainties are given by  $(\delta s^2 + \delta f^2)^{1/2}$ , where  $\delta s$  is the statistical deviation in the repeated measurements and  $\delta f$  is the absolute uncertainty of the difference frequency. The value of  $\delta f$  is given by  $(\delta c^2 + \delta n^2)^{1/2}$ , where  $\delta c$  is the uncertainty of the  $\text{CO}_2$  laser frequency and  $\delta n$  is that of the  $^{15}\text{NH}_3$  laser frequency. In our system,  $\delta c$  is less than 25 kHz, whereas  $\delta n$  is 100–150 kHz. The uncertainty of the difference is dominated by the  $^{15}\text{NH}_3$  frequency uncertainty. In the 6–7-THz region,  $\delta s$  and  $\delta f$  make comparable contributions to the total uncertainty of the measured frequency; however, above 7 THz,  $\delta s$  dominates the total uncertainty because of the lower signal-to-noise ratio and a larger Doppler width.

Both reduced MIM diode efficiency and reduced detector sensitivity are responsible for the poor signal-to-noise ratio above 7 THz. The MIM diode efficiency decreases as the generated FIR frequency increases, probably because of this diode's finite capacitance. The efficiency is estimated from an analysis based on the equivalent circuit of a MIM diode.<sup>21</sup> A typical capacitance of  $2.5 \times 10^{-3} \text{ pF}$  reduces the diode efficiency at 8 THz to  $\sim 10\%$  of that at 3 THz. Typical FIR power of  $\sim 1 \text{ nW}$  is provided at 8 THz. We have observed spectra of  $\text{CH}_3\text{OH}$  up to THz with the Ge:Ga photoconductive detector whose sensitivity peaks near 3 THz and drops to  $\sim 10\%$  at 8 THz.

We used third-order generation, in which tunable FIR radiation is obtained with two  $\text{CO}_2$  lasers plus microwave sidebands, because of its wide tuning range ( $\pm 20 \text{ GHz}$ ). However, second-order generation, in which tunable FIR radiation is obtained with a tunable-waveguide  $\text{CO}_2$  laser without the microwave sidebands, may provide higher-frequency operation because it produces several times as much FIR power. Furthermore, a Ge:Be photoconductive detector is more sensitive in the 6–10-THz region.<sup>22</sup> With second-order generation and a Ge:Be detector, this TuFIR technique should be applicable up to  $\sim 10 \text{ THz}$ .

Table 1. Observed Frequencies of  $\text{CH}_3\text{OH}$

Transition Symmetry	$(n', K', J') \leftarrow (n'', K'', J'')$	Laser Lines		Observed Frequency (MHz)	
		$\text{CO}_2$	$^{15}\text{NH}_3$	Previous Work <sup>a</sup>	This Work <sup>b</sup>
$A$	$(2, 8, 18) \leftarrow (1, 7, 17)$	$R(6)_{\text{II}}$	$aP(4, 0)$	6 567 405	6 567 405.01(32)
$A$	$(3, 6, 6) \leftarrow (2, 5, 5)$	$R(36)_{\text{II}}$	$aP(4, 0)$	7 134 698 <sup>c</sup>	7 134 675.03(73)
$E$	$(1, -4, 9) \leftarrow (0, -3, 9)$	$R(36)_{\text{II}}$	$aP(4, 0)$	7 134 736 <sup>c</sup>	7 134 730.84(117)
$A$	$(1, 5, 12) \leftarrow (0, 4, 11)$	$R(30)_{\text{II}}$	$aP(5, 3)$	7 658 036	7 658 033.06(76)
$E$	$(1, -4, 15) \leftarrow (0, -3, 14)$	$R(42)_{\text{II}}$	$aP(5, 3)$	7 851 010	7 851 003.94(75)

<sup>a</sup>Wave numbers in Ref. 20 are converted into frequencies for comparison.

<sup>b</sup>The numbers in parentheses are the estimated  $1\sigma$  uncertainties in units of the last quoted digits.

<sup>c</sup>These two transitions are not well resolved in the Fourier-transform spectra, which could explain the large deviation from the present measurements.

The authors thank Lew Mullen for his technical support. This research was supported by NASA contract W-18, 913. M. Tachikawa is grateful to the Telecommunication Advancement Foundation for providing the funds for his study at the National Institute of Standards and Technology.

## References

1. K. M. Evenson, in *Atomic, Molecular, & Optical Physics Handbook*, G. W. F. Drake, ed. (American Institute of Physics Press, Woodbury, New York, 1996), p. 473.
2. G. Moruzzi, P. Riminucci, F. Strumia, B. Carli, M. Carlotti, R. M. Lees, I. Mukhopadhyay, J. W. C. Johns, B. P. Winnewisser, and M. Winnewisser, *J. Mol. Spectrosc.* **144**, 139 (1990).
3. D. D. Bićanić, B. F. J. Zuidberg, and A. Dymanus, *Appl. Phys. Lett.* **32**, 367 (1978).
4. K. Liu, J. D. Cruzan, and R. J. Saykally, *Science* **271**, 929 (1996).
5. G. A. Blake, K. B. Laughlin, R. C. Cohen, K. L. Busarow, D.-H. Gwo, C. A. Schmuttenmaer, D. W. Steyert, and R. J. Saykally, *Rev. Sci. Instrum.* **62**, 1693 (1991).
6. C. A. Schmuttenmaer, R. C. Cohen, N. Pugliano, J. R. Heath, A. L. Cooksy, K. L. Busarow, and R. J. Saykally, *Science* **249**, 897 (1990).
7. K. M. Evenson, D. A. Jennings, and F. R. Petersen, *Appl. Phys. Lett.* **44**, 576 (1984).
8. I. G. Nolt, J. V. Radostitz, G. DiLonardo, K. M. Evenson, D. A. Jennings, K. R. Leopold, M. D. Vanek, L. R. Zink, A. Hinz, and K. V. Chance, *J. Mol. Spectrosc.* **125**, 274 (1987).
9. F. Matsushima, H. Odashima, D. Wang, S. Tsunekawa, and K. Takagi, *Jpn. J. Appl. Phys.* **33**, 315 (1994).
10. T. D. Verberg and K. M. Evenson, *IEEE Trans. Instrum. Meas.* **42**, 412 (1993).
11. F. Matsushima, K. M. Evenson, and L. R. Zink, *J. Mol. Spectrosc.* **164**, 517 (1994).
12. H. Odashima, F. Matsushima, K. Nagai, S. Tsunekawa, and K. Takagi, *J. Mol. Spectrosc.* **173**, 404 (1995).
13. K. J. Siemsen and J. Reid, *Opt. Lett.* **10**, 594 (1985).
14. A. G. Maki, C.-C. Chou, K. M. Evenson, L. R. Zink, and J.-T. Shy, *J. Mol. Spectrosc.* **167**, 211 (1994).
15. M. Tachikawa and K. M. Evenson, *Opt. Lett.* **21**, 1247 (1996).
16. L. R. Zink, F. S. Pavone, R. Meucci, M. Prevedelli, and M. Inguscio, *Opt. Commun.* **77**, 41 (1990).
17. J. L. Hall, H. G. Robinson, T. Baer, and L. Hollberg, in *Advances in Laser Spectroscopy*, F. T. Arecchi, F. Strumia, and H. Walther, eds. (Plenum, New York, 1981), p. 99.
18. H. Odashima, M. Tachikawa, L. R. Zink, and K. M. Evenson, "Heterodyne frequency measurement of a sub-Doppler stabilized mid-infrared  $^{15}\text{NH}_3$  laser," *J. Mol. Spectrosc.* (to be published).
19. C. Freed and A. Javan, *Appl. Phys. Lett.* **17**, 53 (1970).
20. G. Moruzzi, B. P. Winnewisser, M. Winnewisser, I. Mukhopadhyay, and F. Strumia, *Microwave, Infrared and Laser Transitions of Methanol* (CRC, Boca Raton, Fla., 1995), Table 9.2.
21. I. H. Odashima, K. Yamamoto, F. Matsushima, S. Tsunekawa, and K. Takagi, *IEEE J. Quantum Electron.* **32**, 350 (1996).
22. E. E. Haller, *Infrared Phys. Technol.* **35**, 127 (1994).